UNITED IMAGING

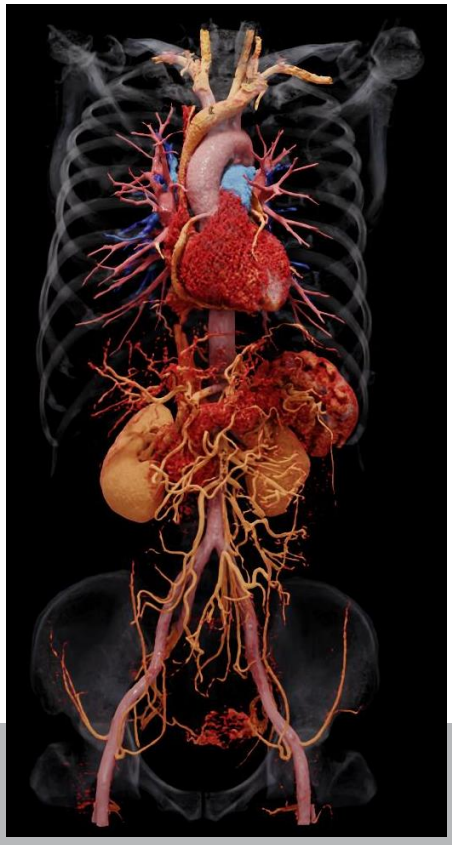

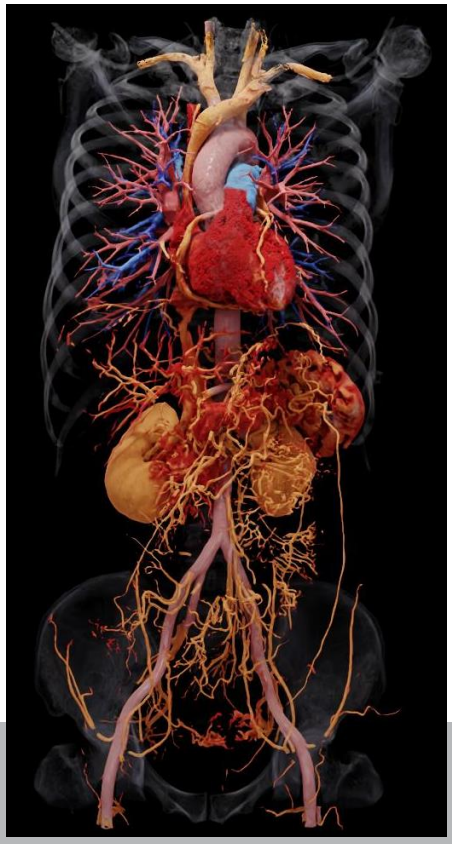

AIIR

The World's Pioneering CT Image Reconstruction Technology

TECHNICAL WHITE PAPER
VERSION 2

Contents

Introduction

United Imaging Healthcare (UIH) has pioneered groundbreaking technology in computed tomography image reconstruction that seamlessly integrates the benefits of cutting-edge deep learning technology – a subset of Artificial Intelligence (AI) – with the power of model-based iterative reconstruction (MBIR).The Artificial-Intelligence Iterative Reconstruction (AIIR) technology stands out as the most advanced CT image reconstruction architecture which allows for the delivery of superior image quality.

Reconstruction by AIIR involves an optimization process similar to Model-Based Iterative Reconstruction (MBIR), from the projection domain to the image domain.Throughout the iterative loop of forward and backward projections, AIIR maintains factors for modeling optics, noise, anatomy, and physics statistics. It also incorporates deep learning based de-noising technology to replace the role of traditional regularization of MBIR in the optimization reconstruction process.UIH's AIIR can reduce image noise, suppress streak and cone-beam artifacts, increase spatial resolution and improve low contrast detectability.AIIR allows for the reduction of radiation dose required for a diagnostic CT image while maintaining image quality.

In this white paper, we will first give a brief introduction of the characteristics and challenges of traditional CT reconstruction technologies.Next, the design of AIIR will be explained, including the data training of the deep learning de-noising engine and workflow. Then, the core advantages of AIIR in clinical applications will be introduced.Finally, the reconstruction performance of AIIR will be presented in both phantom test and clinical cases.

Challenges of Conventional Filtered Back Projection, Hybrid Iterative, and Model-Based Iterative Reconstruction

Historically, filtered back projection (FBP) has been the preferred CT reconstruction algorithm.However, with a lower radiation dose, the FBP results contain higher noise. As a result, the image quality and capability to provide accurate diagnosis are degraded.In addition, because the anatomy of the human body is generally elliptical in the cross-section (especially in pelvis and shoulder), the attenuation of x-ray at different view angles varies.With a constant exposure strength, significant streak artifacts along the lateral direction are often distinct in FBP images. Moreover, reconstruction with FBP is a one-way approximation process, so some artifacts due to partial data insufficiency, like cone-beam artifacts cannot be avoided.

To reduce the image noise and artifact in the traditional FBP reconstruction, a hybrid iterative reconstruction method was introduced.This method is based on the FBP architecture, while applying iterative noise reduction algorithms in both the projection domain and the image domain to reduce the streak artifacts and the image noise. However, due to the intrinsic property of FBP, the ability to reduce noise, streak artifacts,and core-beam would be limited with further dose reduction.

To overcome the limitation, the model-based iterative reconstruction (MBIR) was proposed.MBIR is a fully iterative reconstruction technique that can incorporate a sophisticated model to describe the data acquisition process and a general prior term to regularize the final reconstruction.Images are reconstructed by minimizing an objective function that includes a data-fidelity term involving a system model and a statistical noise model, and a regularization term that stabilizes the image properties [1].

Introduction

The system model can describe the nonlinear, polychromatic nature of the measured data set. The statistical noise model takes photon statistics and electronic noise into consideration. The prior term describes the general form or properties of the reconstructed images and provides tunable image quality trade-offs [2]. In combination, these models enable MBIR to break through the inherent limitations of the traditional FBP method and the hybrid iterative method, so that it can fundamentally eliminate the noise problem of the data [3], and retain the original high-frequency details of the image as much as possible while eliminating the high-frequency noise of the image. Moreover, with a well-defined prior, the missing sampling component with a cone-beam geometry can be approximated and the cone-beam artifacts can be well suppressed. This ability is unique to MBIR methods compared with the iterative FBP methods.

Despite the high potential in image quality improvement, the application of MBIR methods still has its challenges. First and foremost, the algorithm architecture complexity of MBIR is higher compared with FBP and hybrid iterative reconstruction methods. Specifically, the regularization is usually difficult to design and greatly depends on the experience of the developer. Secondly, different regularization strengths can lead to significant differences in image quality. With too high regularization strength, the MBIR images can have unnatural "plastic texture" and eliminate fine structures that may be crucial. Moreover, due to the combination of data-fidelity term and prior-term, MBIR reconstructions appear to be increasingly data-dependent. With the same regularization design and strength, the image quality strongly depends on the scan protocol, patient anatomy, and location of interests. In addition, compared with FBP and hybrid iterative reconstruction methods, MBIR methods have a slower reconstruction speed due to the complex iterative process that involves multiple forward and backward projection computations, limiting the availability for CT scanning in high patient volume settings.

To develop a robust and fast MBIR method that can be deployed in the clinical routine, we propose an adaptive regularization term that eliminates the unnatural image texture and accelerates the overall reconstruction speed.

Development of Deep Learning-Based Image Reconstruction

Deep learning as a sub-category of AI technology, has been developing rapidly. Recently, researchers have incorporated deep learning technology into CT reconstruction and demonstrated impressive improvement in image quality as well as reconstruction speed [4-6]. This data-driven reconstruction method demonstrates exceptional noise reduction capabilities, effectively ushering in a new era of low-dose image reconstruction. The basic principle of a mainstream deep learning-based image de-noising approach is as follows: During the training process, pairs of low-dose images with compromised image quality and normal-dose images with high quality serve as inputs and output labels to train a deep neural network (DNN). The objective is to optimize the numerous parameters in the DNN. This optimized DNN is then used as a fixed model in the application process, where the network can process any low-dose images to reduce the noise while maintaining the fine structures.

Now that this deep learning technology has reached a high level of maturity, the time is right to explore an innovative reconstruction technology that combines those latest advances with the advantages of MBIR.

AIIR: The World's First CT Reconstruction Algorithm that Combines Deep Learning and MBIR

The objectives behind designing high-performance CT reconstruction algorithms include obtaining high-quality CT images with lower noise, higher contrast resolution, higher spatial resolution, fewer artifacts, and more natural anatomical structures and noise texture, all while reducing the dose.

After years of diligent research and development, UIH is proud to present AIIR. The world's first CT reconstruction algorithm which combines deep learning technology and MBIR algorithm. Originating from a unique architecture, AIIR utilizes the advantages of both MBIR and deep learning technologies. Using the same iterative framework as a conventional MBIR method, AIIR adopts a realistic statistical CT forward model and compares the synthetic measurements based on the current image estimates with the measurements. Incorporating a pre-trained deep prior, AIIR inherits the good natural effect of deep learning de-noising network to further improve the image quality while maintaining the natural noise texture. AIIR is a breakthrough in CT reconstruction technology and one of the most advanced reconstruction technologies in the world (Figure 1).

Figure 1. The Generations of CT Reconstruction Technology.

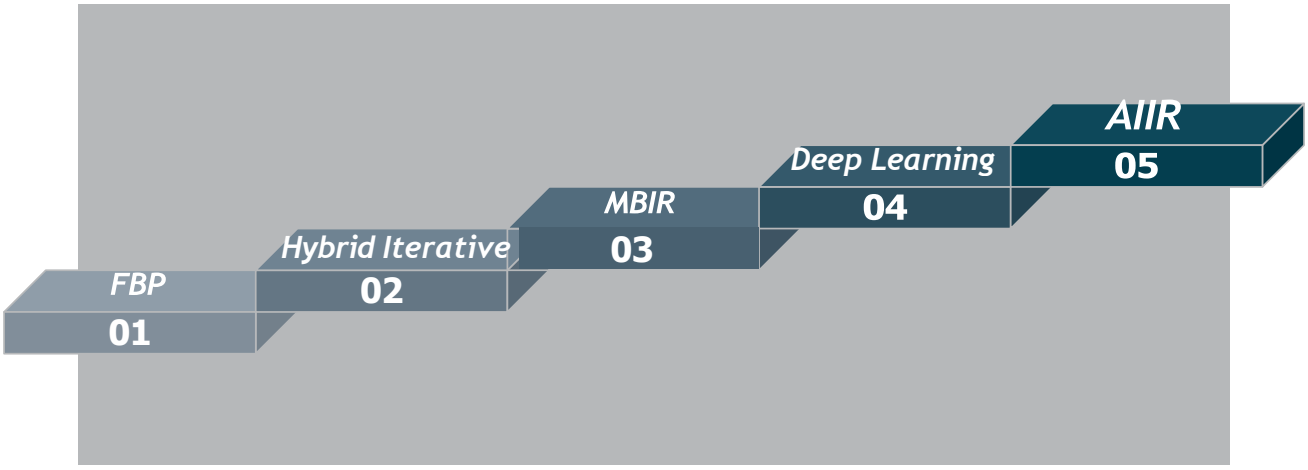

AIIR Overcomes the Limitation of MBIR

The basic principle of the MBIR algorithm can be described using the following optimization problem:

Equation 1:

$$U^* = argmin_U \left(\|AU - Y\|_W^2 + \beta R(U) \right)$$

Equation 1 is the objective function that includes the data fidelity term $\|AU - Y\|_W^2$ and the regularization term $\beta R(U)$ [7].

The CT image is denoted with U and the line-integrals is denoted with Y; a well calibrated system matrix **A**, the relationship between the mean of the image U and the line-integrals **Y** can be modeled as **Equation 2.**

Equation 2:

$$\bar{Y} = A\bar{U}$$

The data fidelity term is derived as the marginal likelihood function presuming that the noisy line-integrals follow a Gaussian distribution with a covariance matrix **W**.

In practice, the regularization term $R(U)$ is difficult to design.The regularization term can be considered as a prior information about the image U.Since the specific type of regularization function $R(U)$ is designed manually, it can only focus on very simple description of clinical image characteristics with a limited number of parameters to adapt.Due to the limitation in the conventional design mentioned above, the performance of the widely used norm-based regularization functions will result in unnatural image structures, such as plastic-looking appearances, usually more severe when the scan dose is lower.This is a major limitation of MBIR for clinical low dose CT applications.

Deep learning technology is a good solution to address the challenges of manual regularization design. UIH's AIIR is a new perspective which replaces the handcraft regularization term with a data driven trained deep learning model.

A deep-learning-based regularization function has two main advantages over conventional regularization based on norms.First and foremost, a deep learning network such as a CNN usually has millions of parameters.The enormous number of parameters, impossible to set manually in traditional regularization functions, provide the model with almost boundless potential to describe more complex characteristics of clinical images.Second, the deep learning-based regularization model was trained with high quality clinical images, accepted by radiologists as the training target or label.The model learned to differentiate the signal from noise and describe the image characteristics from itself.It has the power to describe the image characteristics with abstract features that cannot be pre-defined in the traditional MBIR regularization function. As a result, the trained network will provide images that directly match the quality requirements of the users.While solving the limitations of MBIR, deep learning also has the capability to reduce image noise, which can further improve the quality of the reconstructed images [10].

The Workflow of AIIR

The architecture of AIIR is based on the framework of MBIR, in which a deep learning de-noising engine is introduced as the regularization process to remove the limitation of conventional MBIR.

As one core part of AIIR, the data-fidelity term considers multiple models to fully describe the system properties including a system optics model, a detector model and a quantum statistical model of each specific scan during data collection.At each iteration loop, the estimated images are transformed into projection data and compared with acquired projection data, then updated via forward and backward projection.During this process, detailed information from the raw projection data can be added to the image, so that the anatomic and pathological information can be preserved in the image.

In addition to the data-fidelity term, the deep learning de-noising engine determines the reconstruction performance of AIIR.This is a data-driven method, and its performance largely depends on the training dataset. The training dataset of AIIR which contains millions of high-quality/low-dose image pairs is generated directly from the MBIR methods.This dataset encompasses a wide range of clinical scenarios, including multiple body parts, ages, genders, body types, diverse scan protocols, radiation dose levels, and typical diseases. The large number of cases in the training dataset ensures the network's generalizability and robustness.Figure 2 illustrates the training process of the deep learning de-noising engine.

The diagram of the AIIR optimization algorithm is shown in Figure 3.In each iteration, the AIIR method first seeks to minimize the data-fidelity cost function, and then applies the deep learning de-noising engine to reduce the noise. The image quality improvement increases with more iterations where more detailed information is recovered while the noise is constantly suppressed by the de-noising engine.The iterative process is finished when the reconstructed image meets clinical requirements.

Altogether with the advanced design concept mentioned above, the AIIR has demonstrated outstanding reconstructed image quality in many aspects such as noise reduction, excellent low-contrast detectability, ultra-high spatial resolution, and artifact-free image performances.

The Workflow of AIIR

Figure 2. Deep Learning De-Noising Engine Training Process

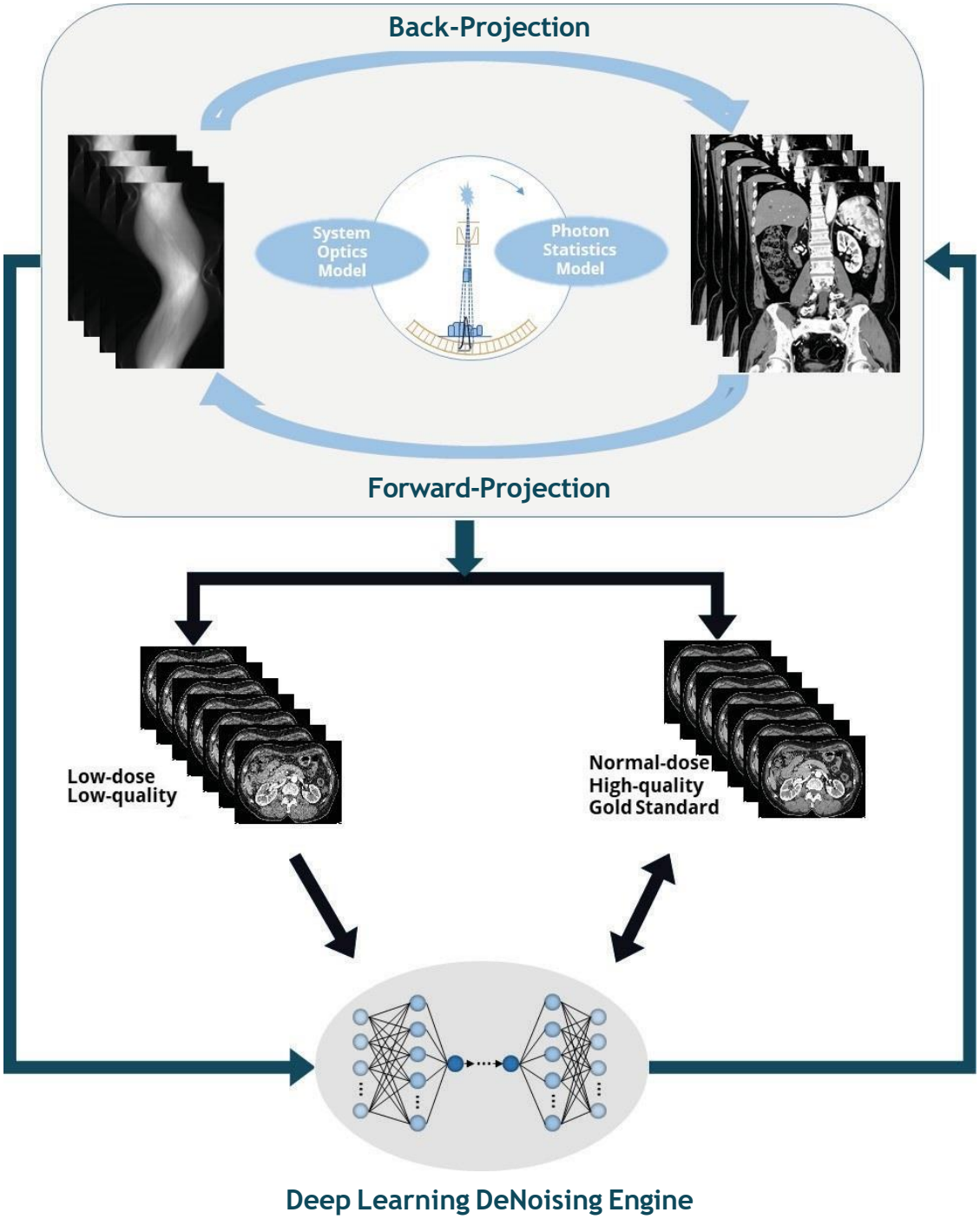

The Workflow of AIIR

Figure 3. AIIR Reconstruction Workflow

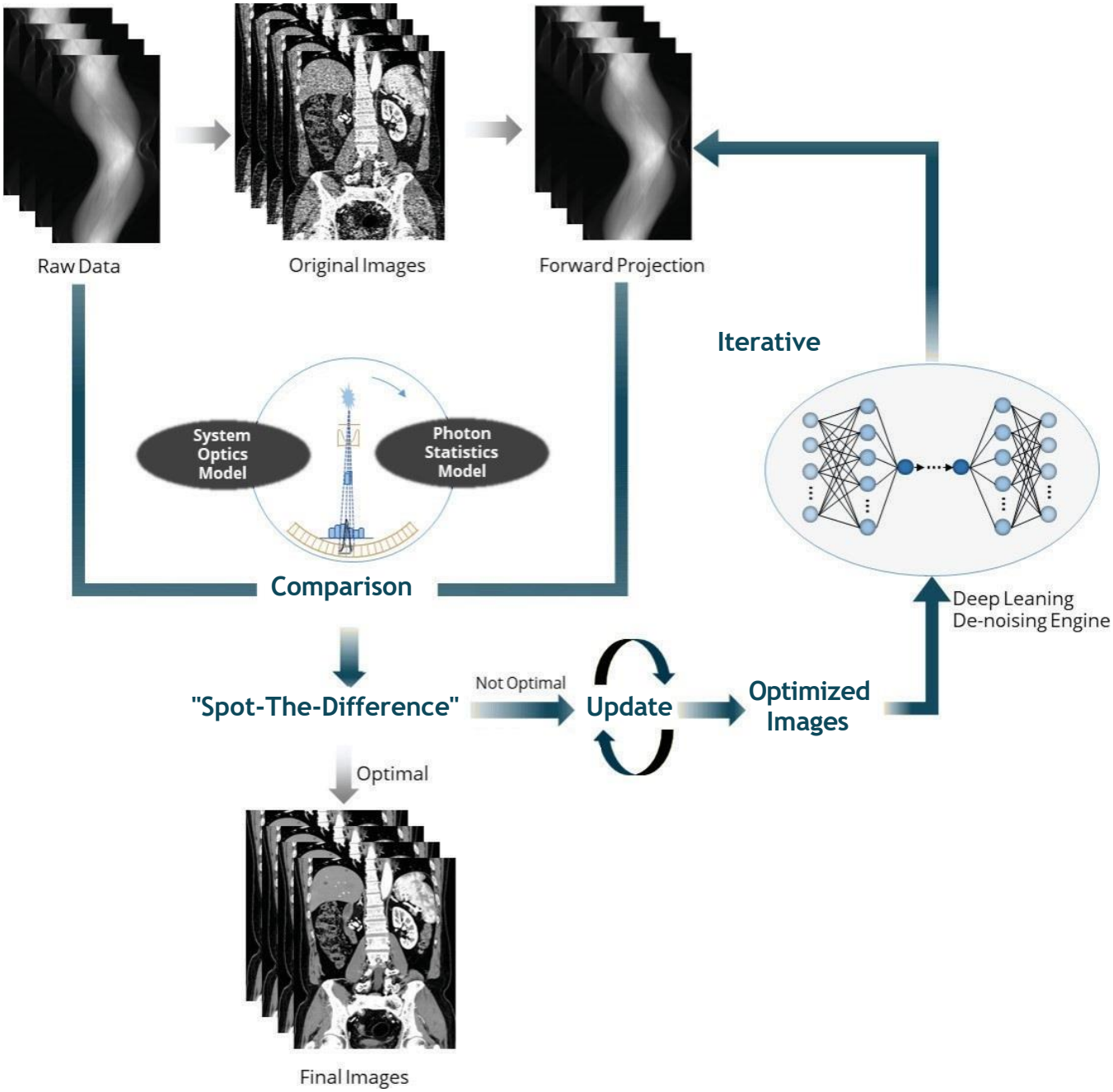

Excellent Performance in Noise Reduction

Compared with the traditional FBP and hybrid iterative reconstruction, AIIR shows excellent noise reduction capability. This was first demonstrated with a water phantom test, where a water phantom of 320 mm diameter was scanned with 120 kV at various dose levels from 10 mAs up to 400 mAs. We then reconstructed the images using FBP, Hybrid IR, and AIIR. The reconstructed images at a high dose level (400 mAs) and a low dose level (15 mAs) are shown in Figure 4. At both dose level, AIIR exhibits the best noise reduction capability compared with FBP or Hybrid IR.

We further computed the noise magnitude in a centered ROI for the three different methods at each dose levels. Figure 5 summarizes the measured noise for the different reconstruction methods. From the noise curves we observe that the AIIR shows the minimal noise level compared to FBP or Hybrid IR over the range of radiation dose. This difference is more distinct at low dose levels, where AIIR can reduce the noise by up to 90% compared with FBP.

Figure 4. Reconstructed Images and STD Values of 320 mm Water Phantom Under Different Reconstruction Methods

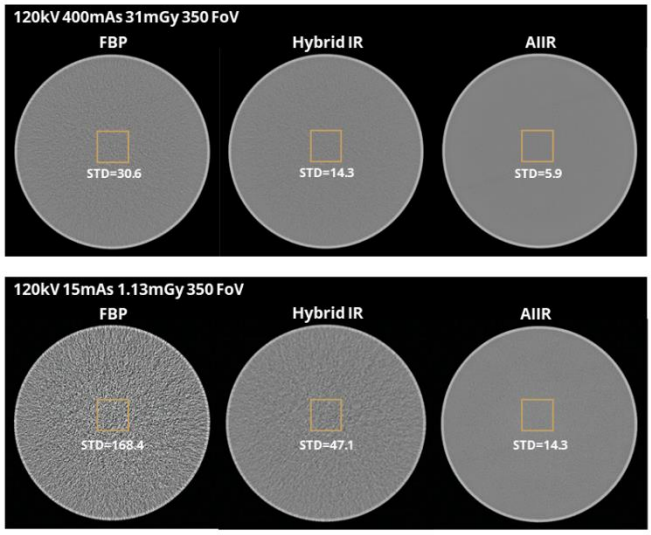

Especially at the15 mAs, which is the "limit" dose for the 320 mm water phantom, the reconstructed image under AIIR still maintains the ultra-low noise.

Figure 5. Curves of Noise with Dose for Different Reconstruction Methods

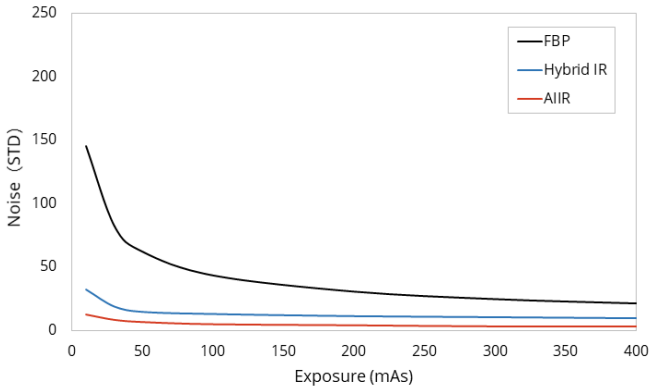

The black, blue and red curves represent the noise levels of FBP, Hybrid IR and AIIR, respectively.

Ultra-low-dose Imaging and Low-contrast Detectability Improvement

Radiation exposure remains a paramount consideration in the advancement of CT Technology.Indeed, every aspect of CT protocols-from scan strategy to reconstruction algorithms-plays a pivotal role in optimizing the balance between image quality and the potential risks of radiation. AIIR's advanced framework helps reconstruct images at ultra-low doses and improve the low-contrast detectability (LCD) of images, outperforming the other clinically available reconstruction methods in ultra-low-dose imaging [11].

We used a model observer LCD evaluation method [12] to evaluate the capability of AIIR for dose reduction and LCD improvement.A CCT189 MITA CT IQ low contrast phantom (The Phantom Laboratory, Salem, NY) was used for evaluation.It contained four rods with different diameters and contrasts.The phantom was scanned with 120 kVp at different dose levels (CTDIvol = 6.40/0.64 mGy).Images were reconstructed using FBP and AIIR. The Channelized Hotelling Observer (CHO) [13] was used to assess the LCD. The Receiver Operating Characteristic (ROC) curves and the Area Under the ROC Curve (AUC) values were calculated to compare the LCD performance between FBP and AIIR.

From the ROC curves and the AUC values shown in figure 6, one can observe that the LCD performance of AIIR at ultra-low dose (1/10 of the normal dose) is better than FBP at the same dose level and comparable with FBP results at normal dose level.This indicates that AIIR can reduce the dose up to 90% compared with FBP at the same LCD.

To further evaluate the performance of LCD, the Catphan 700 phantom was scanned with the head protocol with 120kV 350mAs 48mGy. Images were reconstructed with a slice thickness of 0.5 mm individually using FBP, Hybrid IR, and AIIR, shown in Figure 7. We can see that AIIR improves the LCD compared with FBP and Hybrid IR at the same dose level.

Ultra-low-dose Imaging and Low-contrast Detectability Improvement

Figure 6. Evaluation of Dose Reduction and LCD Improvement Capability of AIIR.

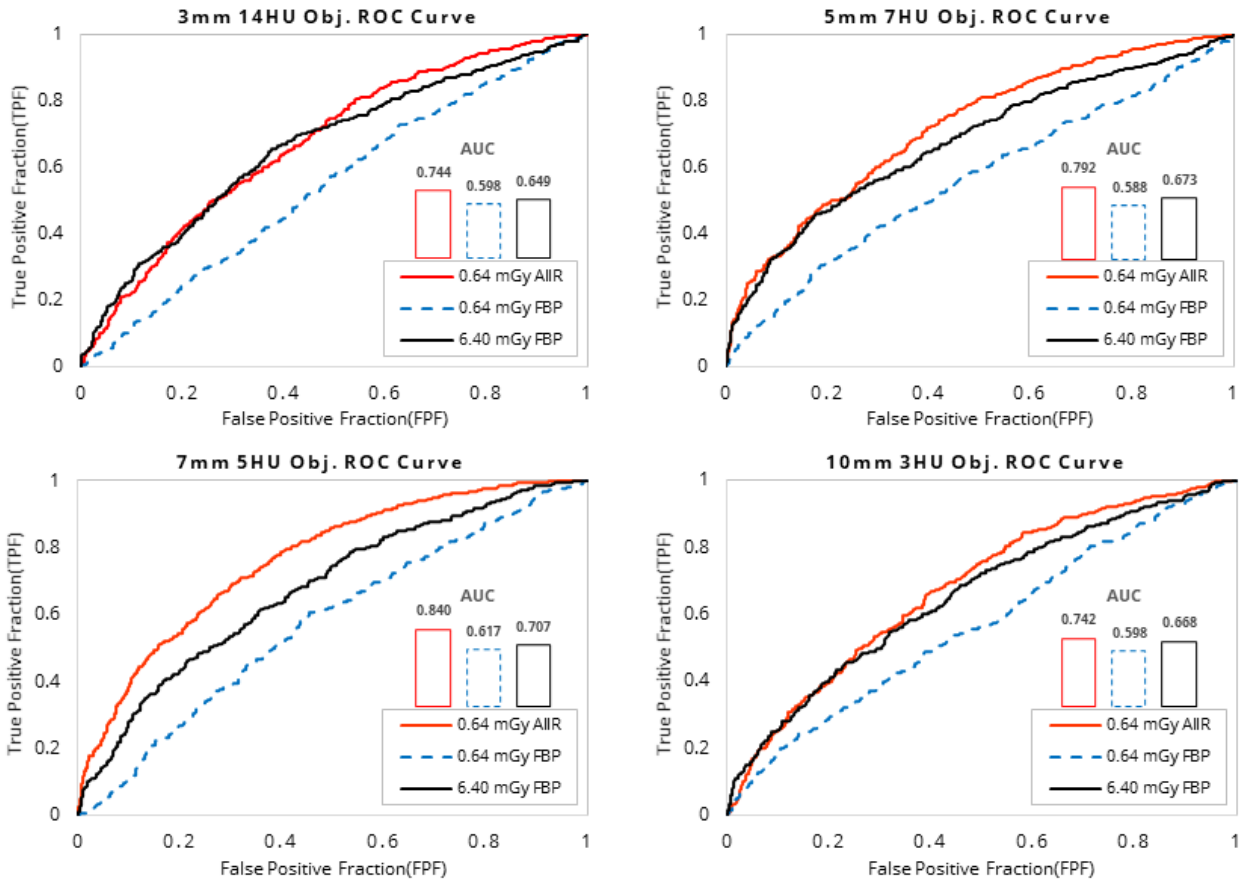

The ROC curves and AUC values of FBP at normal dose, FBP at low dose, and AIIR at low dose are shown in black, blue, and red, respectively. The higher true positive fraction and AUC value, the better the LCD performance.

Ultra-Low-Dose Imaging and Low-contrast Detectability Improvement

Figure 7a. Catphan 700 Phantom Includes Low-Contrast Module with Different Supra-Slice and Subslice Contrast Targets

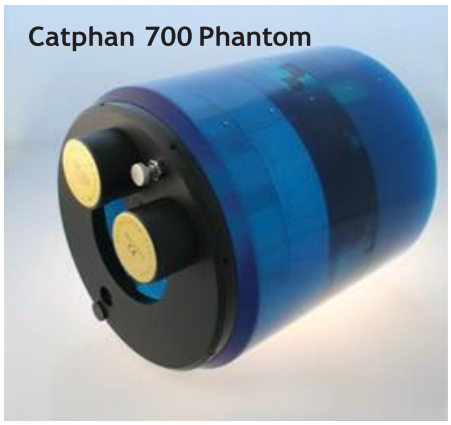

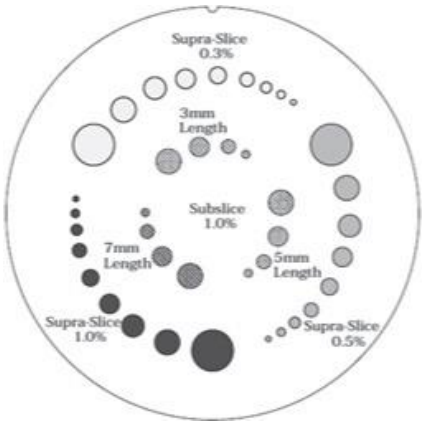

Supra-Slice Target Diameters
2.0 mm, 3.0 mm, 4.0 mm
5.0 mm, 6.0 mm, 7.0 mm
8.0 mm, 9.0 mm, 15.0 mm

Supra-Slice Target Diameters
3.0 mm, 5.0 mm, 7.0 mm, 9.0 mm

Figure 7b. Reconstructed Images of Low-Contrast Module Using FBP, Hybrid IR, and AIIR

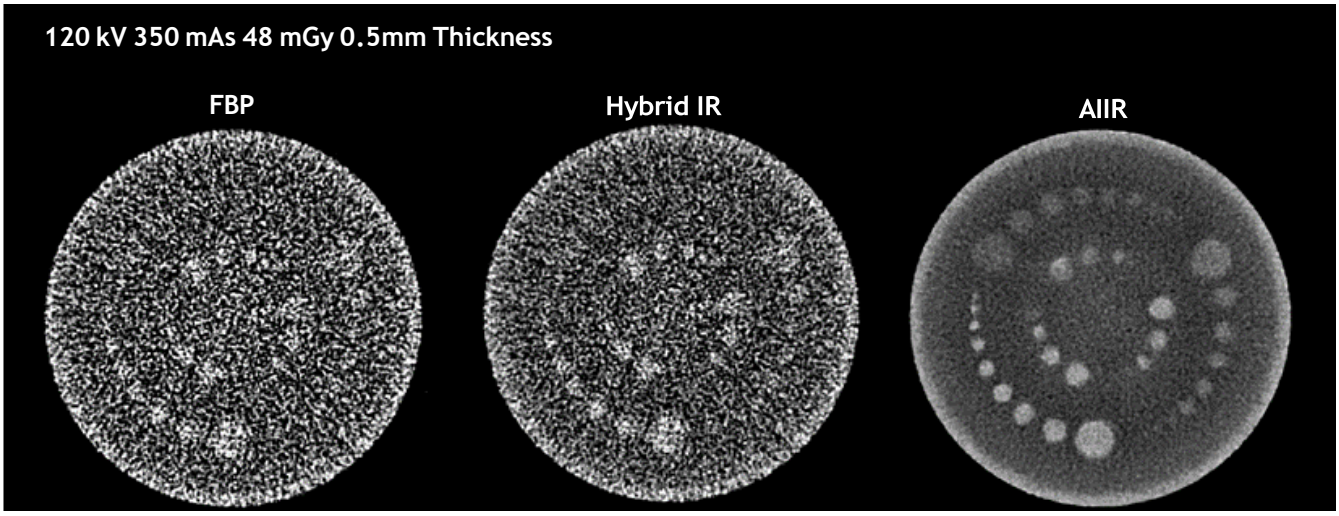

More Details with Improved Ultra-High Spatial Resolution

AIIR inherits the advantages of MBIR method and can reconstruct fine structures.For CT imaging at standard clinical dosage levels, the conventional FBP algorithm may not produce optimal results when imaging certain body parts with intricate and fine structures.AIIR improves spatial resolution and helps the clinicians to identify small lesions.

Figure 8a. CT ACR 464 Phantom

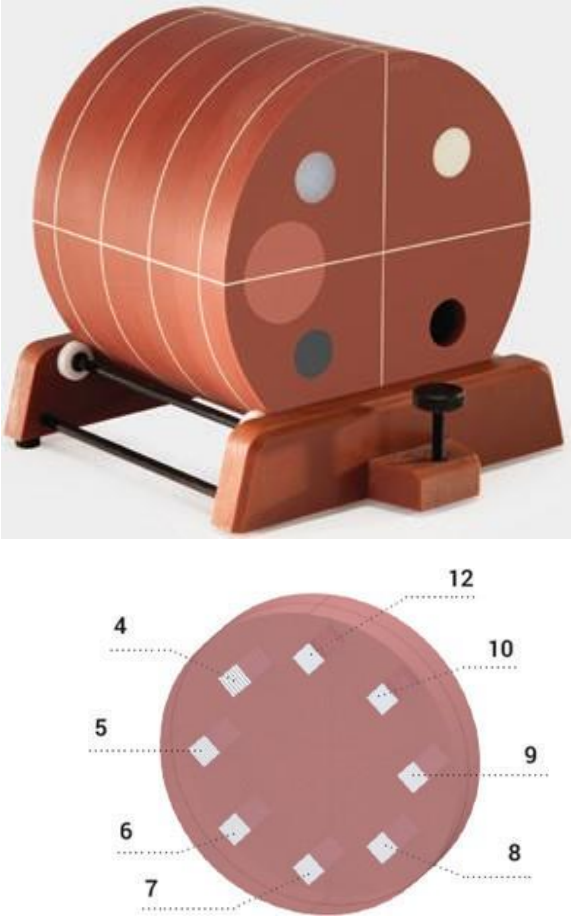

The CT ACR 464 phantom includes a high-spatial resolution module with eight high-contrast line-pair patterns of 4, 5, 6, 7, 8, 9, 10 and 12 line pairs per cm.

To evaluate the spatial resolution properties of AIIR results, we scanned a CT ACR 464 phantom with 120 kV at 300 mAs, namely 23.45 mGy CTDI dose.The phantom images were reconstructed using FBP and AIIR in 512x512 matrices.The reconstructed images of the line-pair phantom shown in Figure 8 demonstrate that AIIR exhibits higher spatial resolution and less noise compared with FBP under the same scanning conditions.

Figure 8b.
120 kV 300 mAs 23.45 mGy 200 FoV 512x512 Matrix

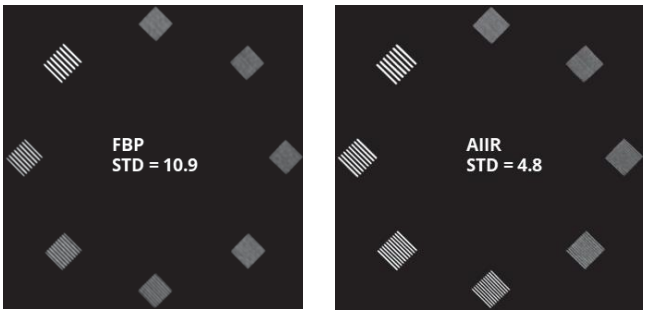

FPB

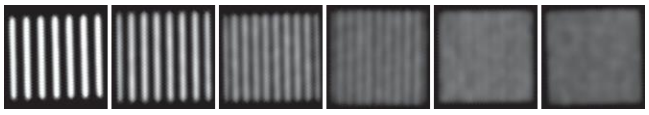

AIIR

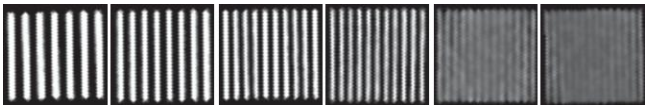

The reconstructed images of CT ACR 464 phantom using FBP and AIIR.One can observe that the line pairs in AIIR reconstructed images are of higher contrast and more differentiable than those in FBP reconstructed images.

Artifact-Free Performance on Streak Artifact Suppression

Streak artifacts are one of the major challenges in high-quality CT image reconstruction, especially in low-dose scans. Because of ultra-high attenuation along the long-axis bone structures, such as the lateral view in shoulder, the measured signals are low and overwhelmed with the noise. This will result in severe directional streak artifacts in the FBP reconstructed CT images (Figure 9a). Hybrid iterative reconstruction methods can somewhat reduce the streak artifacts (Figure 9b), but it is difficult to eliminate all of them.

The issue of streak artifacts can be effectively addressed using AIIR. This is the benefit of the unique AIIR algorithm architecture that combines both the backbone of MBIR and the flesh of data-driven deep-learning technology. The statistical characteristics in raw data, like the inhomogeneity of noise distribution mentioned above, can be gradually filtered out throughout the iterative process of reconstructions, which results in almost complete suppression of the streak artifacts in images (Figure 9c).

In some cases, the patients may not be able to lift their arms and place their arms next to the body. This position can lead to severe streak artifacts in abdominal scans. Figure 10 shows that the AIIR images can properly deal with this class of clinical cases with nearly "streak-artifact-free" performance.

Figure 9. Adult Shoulder CT Images Using Different Reconstruction Methods

Voltage	CTDIvol	DLP	ED	Pitch	Slice thickness	Rotation Speed	Scan type
100kV	5.71mGy	398.6mGy*cm	5.6mSv	1	1.0mm	0.25s	Helical

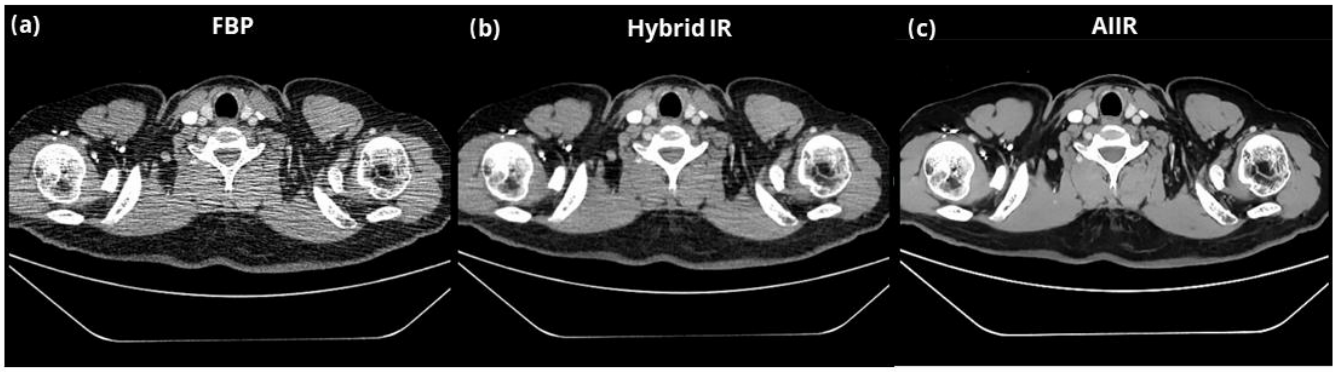

Scan Parameters: 100 kV, CTDIvol=5.71 mGy, pitch=1, slice thickness=1.0 mm, helical scan type

Compared with conventional FBP and Hybrid IR reconstructed CT images, AIIR image shows the advantage of "streak-artifact-free imaging".

Artifact-Free Performance on Streak Artifact Suppression

Figure 10. Adult Abdomen CT Images with Arms Aside Using Different Reconstruction Methods

Voltage	CTDIvol	DLP	ED	Pitch	Slice thickness	Rotation Speed	Scan type
120kV	0.67mGy	113.9mGy*cm	1.6mSv	1.375	0.5mm	0.5s	Helical

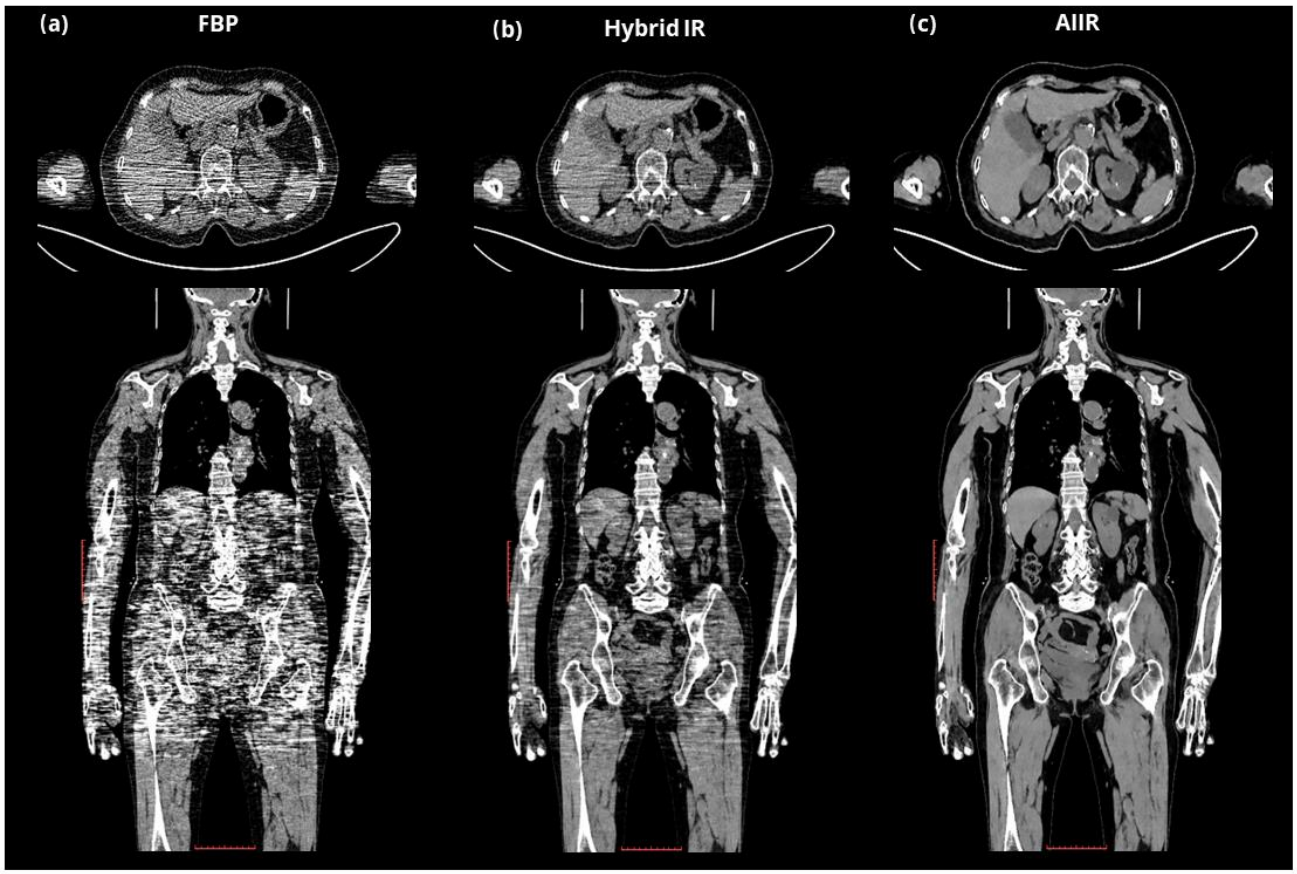

Scan Parameters: 120 kV, CTDIvol=0.67 mGy, pitch=1.37, slice thickness=0.5 mm, helical scan type

The images reconstructed by FBP show severe streak artifacts.Hybrid IR can reduce the streak artifact, yet not enough for diagnostic image quality. AIIR images show the best performance of streak artifact reduction and highest signal-to-noise ratio (SNR) in the image.

Under-sampling Solution with Cone-beam Artifact Suppression

Wide-coverage CT plays an important role in clinical diagnosis. However, such a detector covers a wider cone angle and cannot collect data outside the cone angle. This will result in cone-beam artifacts while the axial spatial resolution decreases from the central plane to the edge. With a data-regularized MBIR, AIIR can reconstruct images with much less cone-beam artifacts than FBP or hybrid iterative images.

The reconstructed images of the compact-disc (CD) phantom shown in Figure 11. The CDs phantom is commonly used as the test for cone-beam artifacts in the industry. If the reconstruction algorithm lacks the ability to eliminate cone-beam artifacts, the reconstructed image would have conspicuous artifacts. In FBP and Hybrid IR images, the CD cross-sections are more and more distorted moving aside from the center plane. The cone-beam artifacts can be reduced in AIIR image, and the coronal image clearly show parallel bars representing the cross-sections of the CDs.

Figure 12 summarizes the cone-beam artifacts suppression in head scans. The cone-beam artifacts appear at the skull base in both FBP images and Hybrid IR images but are completely suppressed in AIIR images. In addition, the AIIR images show less noise, higher LCD, and better contrast between grey and white matter

Figure 11a. The Schematic Diagram of a CDs Phantom

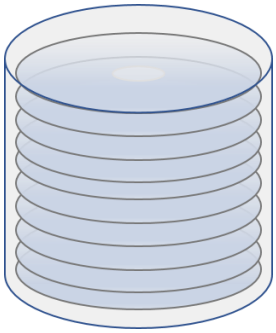

The phantom is made of a regular set of CDs stacked with robber washers to create air gaps between adjacent CDs.

Figure 11b.
120 kV 350 mAs 49.05 mGy 0.5mm Thickness

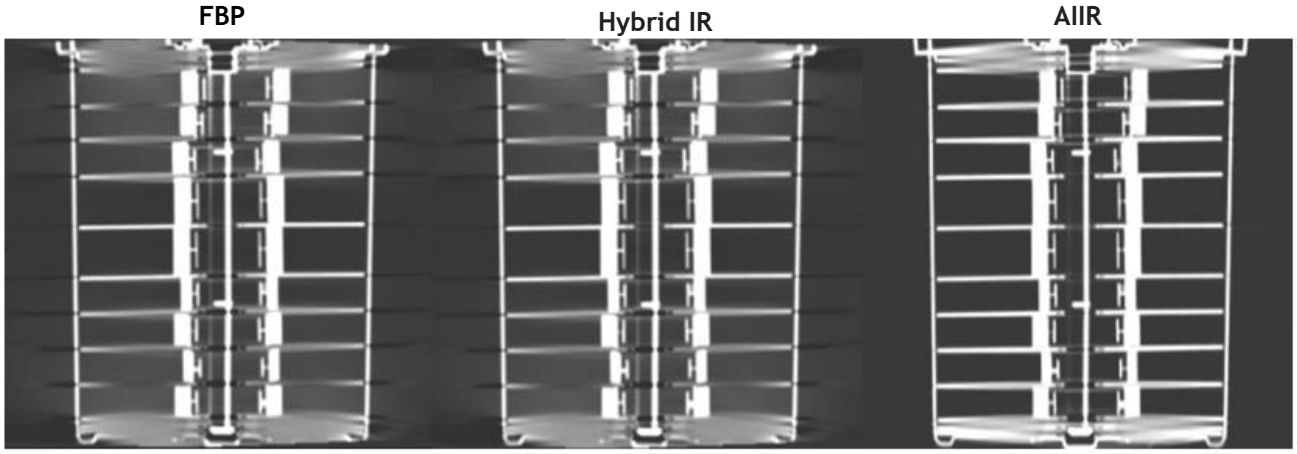

The reconstructed images of CDs phantom using FBP, Hybrid IR and AIIR respectively. Compared with FBP and Hybrid IR image, the cone-beam artifacts can be reduced in AIIR image.

Under-sampling Solution with Cone-beam Artifact Suppression

Figure 12. Adult Head CT Images Using Different Reconstruction Methods

Voltage	Current	CTDIvol	DLP	ED	Slice thickness	Rotation Speed	Scan type
120kV	347mA	48.78mGy	682.9mGy*cm	1.43mSv	0.5mm	0.8s	Axial

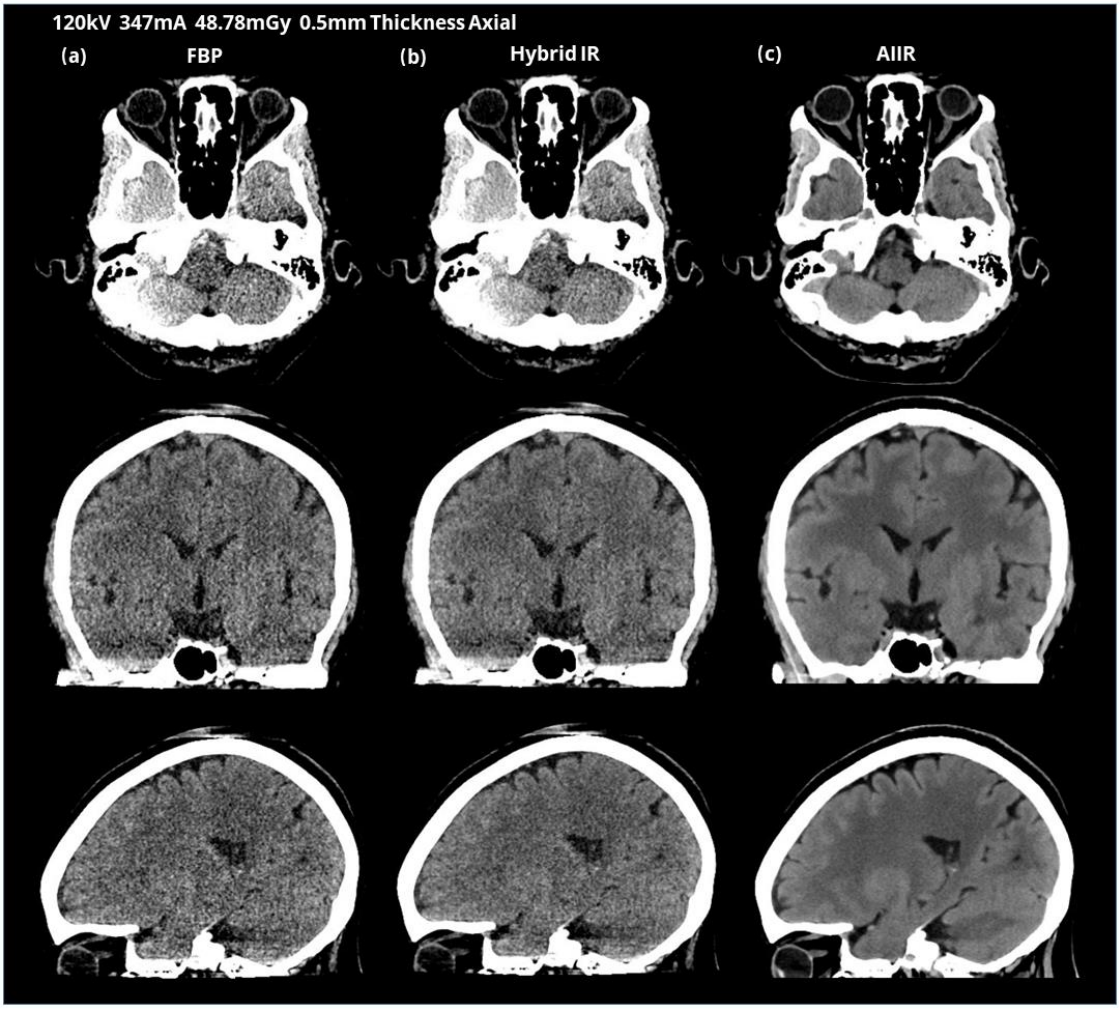

Scan Parameters: 120 kV, CTDIvol=48.78 mGy, slice thickness=0.5 mm, axial scan type

From the top to the bottom show the axial, coronal, and sagittal slices of the reconstructed volumes. From the left to the right show the results of (a) FBP, (b) Hybrid IR, and (c) AIIR, respectively. The FBP images show cone-beam artifacts at the skull base. The Hybrid IR can reduce the cone-beam artifact. AIIR images show the best performance of cone-beam artifact suppression.

Clinical Applications Evidence

To thoroughly assess the effectiveness of the AIIR algorithm in clinical applications, a diverse range of clinical cases have been utilized to showcase its advantages in producing high-quality CT images.

Figure 13 shows a clinical images of an adult chest scan using ultra-low dose (CTDIvol=0.21mGy). According to the ACR 2020 Dose Index Registry (DIR) Executive Summary report [14], 98% dose reduction of a chest scan is realized when compared with the average dose of CTDIvol 12~13 mGy.In this ultra-low dose scanning scenario, the images are reconstructed by FBP, Hybrid IR, and AIIR. In comparison with FBP and Hybrid IR, images reconstructed by AIIR exhibit superior image quality. This is evidenced by the presence of less image noise, and the complete elimination of streak artifacts. Furthermore, the AIIR allows for enhanced visualization of anatomical and pathological details, resulting in images with more realistic image texture and improved diagnostic capabilities. Specifically, the presence of conditions such as emphysema, thickened interlobular septa, and pleura can be more clearly visualized in images reconstructed using the AIIR.

Figure 13. Adult Chest CT Images

Voltage	CTDIvol	DLP	ED	Pitch	Slice thickness	Rotation Speed	Scan type
100kV	0.21mGy	8.11mGy*cm	0.11mSv	1	0.5mm	0.5s	Helical

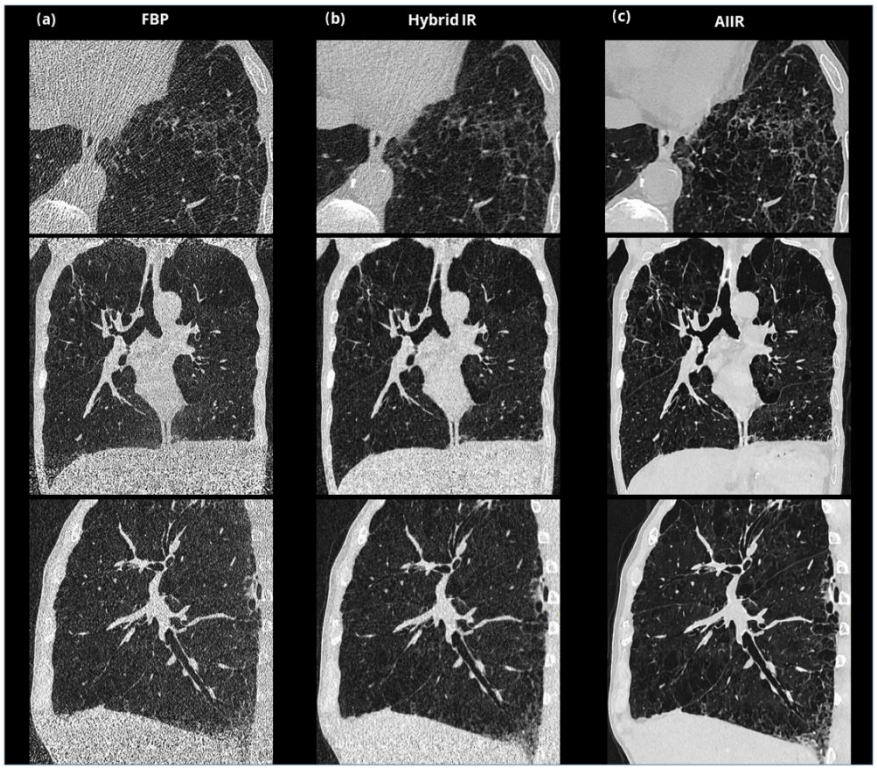

Scan Parameters: 100 kV, CTDIvol=0.21mGy, pitch=1, slice thickness=0.5 mm, helical scan type

From the top to the bottom show the axial, coronal, and sagittal slices of the reconstructed volumes. From the left to the right show the results of (a) FBP, (b) Hybrid IR, and (c) AIIR respectively.

Clinical Applications Evidence

Figure 14 presents a representative example of clinical images obtained from a CT scan of an adult abdomen belonging to an obese patient. The example demonstrates the ability of the imaging reconstruction algorithm to capture detailed anatomic structures, including the abdominal organs and surrounding soft tissue. The images are reconstructed by FBP, Hybrid IR and AIIR under the same scan parameters. When comparing the images produced by FBP and Hybrid IR to those produced by AIIR, it is evident that there is a significant decrease in image noise, an improvement in LCD, a reduction in streak artifacts, an increase in realistic image textures, and a clearer visualization of vascular structures.

Figure 14. Adult Abdomen CT Images

Voltage	CTDIvol	DLP	ED	Pitch	Slice thickness	Rotation Speed	Scan type
120kV	9.36mGy	394.9mGy*cm	5.5mSv	1	0.5mm	0.5s	Helical

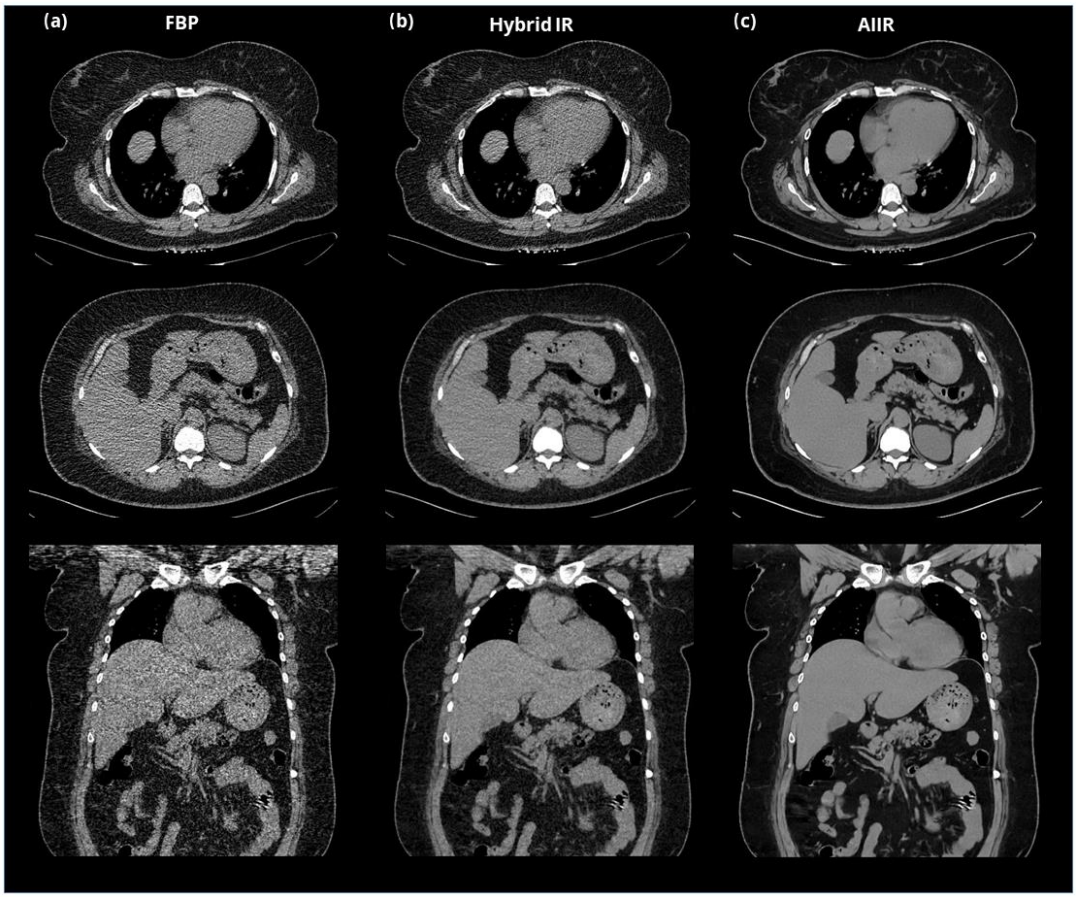

Scan Parameters: 120 kV, CTDIvol=9.36mGy, pitch=1, slice thickness=0.5 mm, helical scan type

From the top to the bottom show the axial, coronal, and sagittal slices of the reconstructed volumes. From the left to the right show the results of (a) FBP, (b) Hybrid IR, and (c) AIIR respectively.

Clinical Applications Evidence

Figure 15 illustrates a representative example of clinical images captured during an adult abdomen and pelvis angiography scan.The images are reconstructed by FBP, Hybrid IR and AIIR under the same scan parameters.At the ultra-low dose, AIIR demonstrated a marked improvement in image quality when compared to FBP and Hybrid IR.Images reconstructed by AIIR exhibited a notable reduction in noise, a significant increase in LCD, a decrease in artifacts, and a more realistic representation of image textures across the axial, coronal, and sagittal planes. Furthermore, the soft tissue structures, small vessels, and even subtle intrahepatic and intrarenal cystic lesions are more clearly visible in the images reconstructed by AIIR.

Figure 15. Adult Abdomen CT Images

Voltage	CTDIvol	DLP	ED	Pitch	Slice thickness	Rotation Speed	Scan type
80kV	2.01mGy	210.5mGy*cm	2.9mSv	1	1.0mm	0.25s	Helical

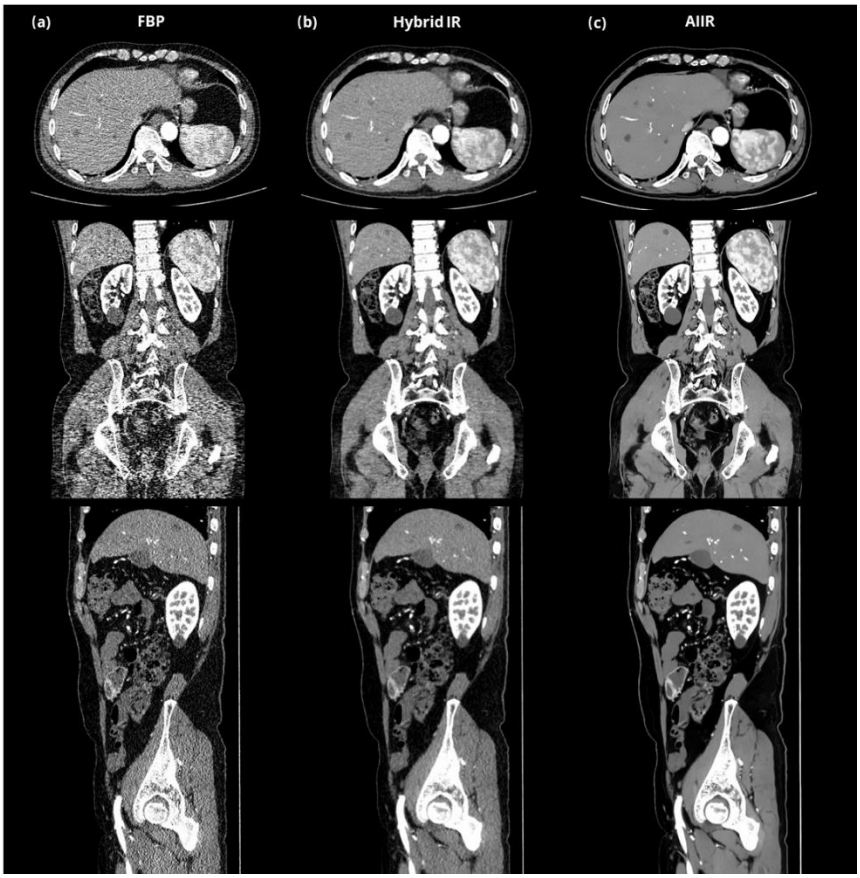

Scan Parameters: 80 kV, CTDIvol=2.01mGy, pitch=1, slice thickness=1.0 mm, helical scan type.

From the top to the bottom show the axial, coronal, and sagittal slices of the reconstructed volumes.From the left to the right show the results of (a) FBP, (b) Hybrid IR, and (c) AIIR respectively.

Clinical Applications Evidence

Figure 16 shows an example of clinical images in an adult abdomen angiography scan.The images are reconstructed by FBP, Hybrid IR and AIIR under the same scan parameters. At the low dose, AIIR exhibits a notable improvement in image quality when compared to FBP and Hybrid IR.The image noise is significantly reduced, resulting in higher spatial resolution and improved visualization of the pulmonary artery dissection.The true and false lumen can be distinguished with greater clarity, allowing for better identification of the origin of the abdominal cavity from the true lumen.

Figure 16. Adult Abdomen Angiography Scanning CT Images

Voltage	CTDIvol	DLP	ED	Pitch	Slice thickness	Rotation Speed	Scan type
100kV	5.71mGy	398.6mGy*cm	5.6mSv	1	1.0mm	0.25s	Helical

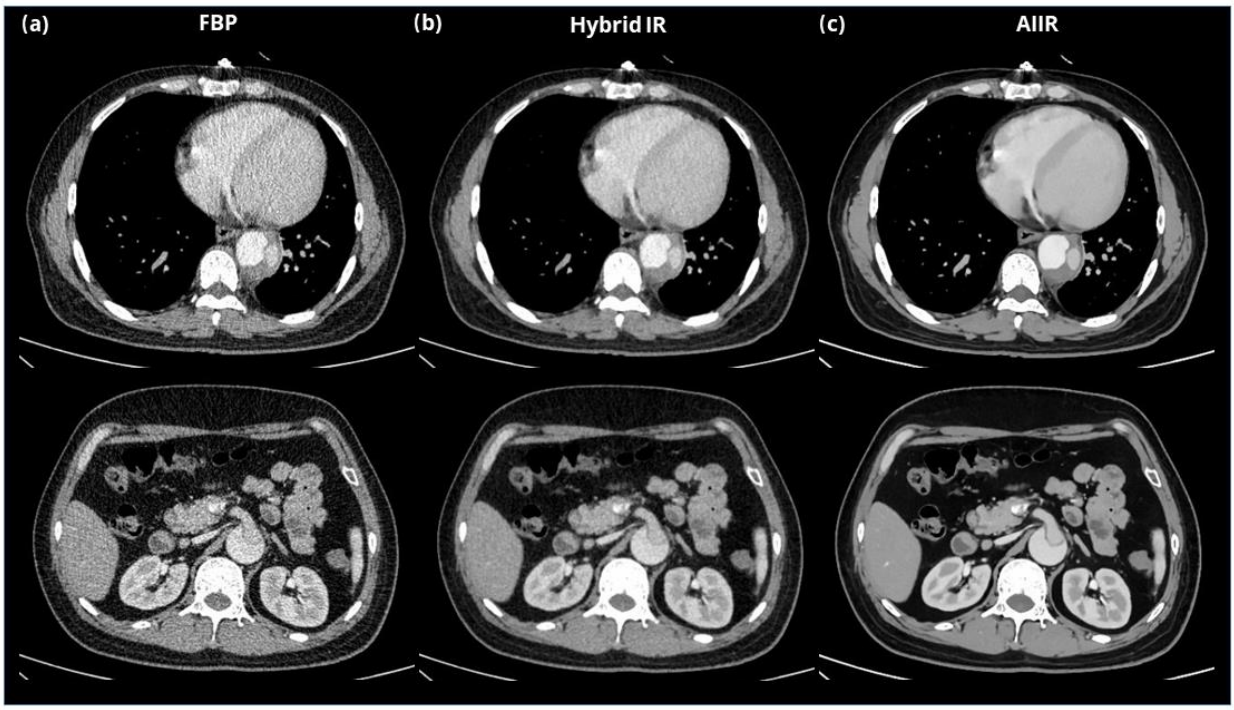

Scan Parameters: 100 kV,CTDIvol=5.71mGy, pitch=1, slice thickness=1.0 mm, helical scan type

From the left to the right show the results of (a) FBP, (b) Hybrid IR, and (c) AIIR respectively.

Clinical Applications Evidence

Figure 17 shows the example of clinical images in an adult head volume perfusion scan. The images are reconstructed by FBP and AIIR under the same scan parameters. Comparing to FBP and Hybrid IR, AIIR demonstrates a notable improvement in image quality. Images reconstructed by AIIR exhibit a marked reduction in noise, a decrease in artifacts, and an improved visualization of the focal cerebral ischemia and cerebral vessels.

Figure 17. Adult Head Perfusion Scanning CT Images

Voltage	Current	CTDIvol	DLP	ED	Total phase	Slice thickness	Rotation Speed	Scan type
80kV	201mA	166.51mGy	2664.1mGy*cm	5.6mSv	19	5.0mm	0.5s	Axial

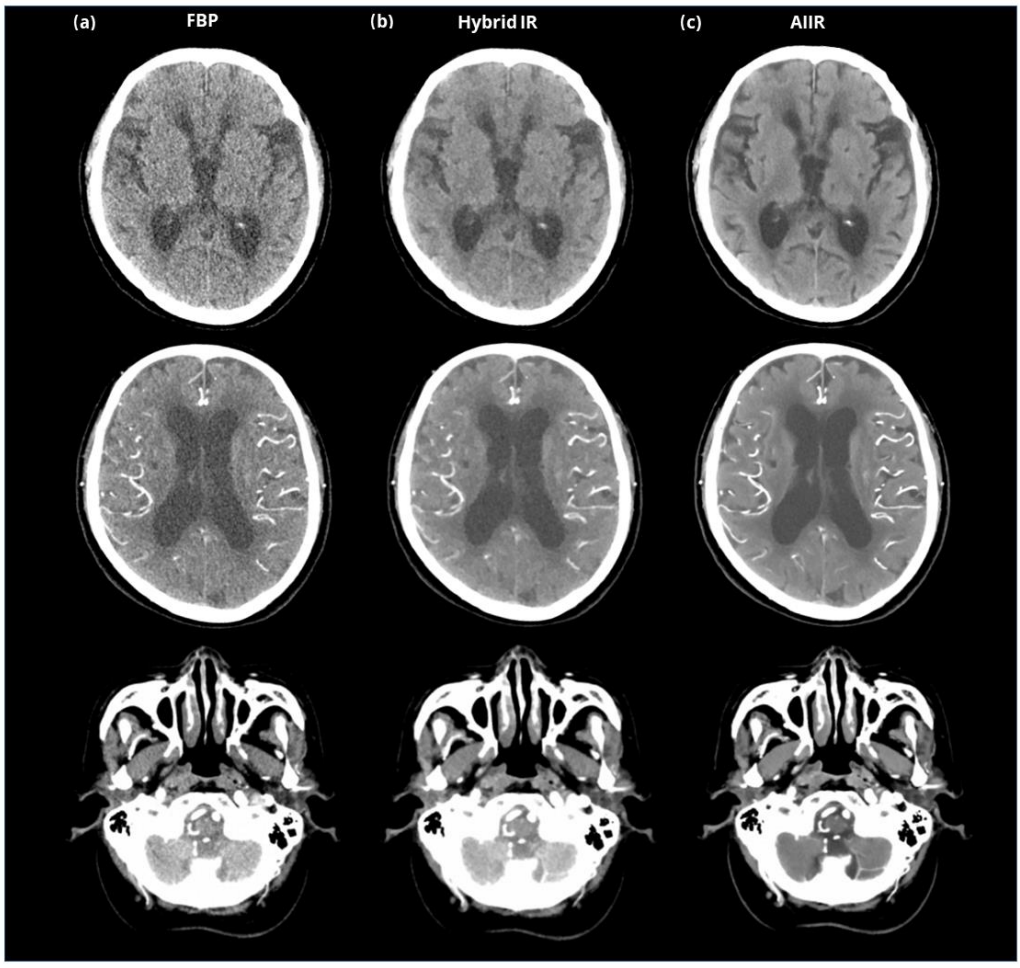

Scan Parameters: 80 kV, CTDIvol=166.51mGy, slice thickness=5.0 mm, axial scan type

From the left to the right show the results of (a) FBP, (b) Hybrid IR, and (c) AIIR respectively.

Clinical Applications Evidence

Figure 18 shows the example of clinical images in an angiography scan of an adult head. The images are reconstructed by FBP and AIIR under the same scan parameters. In comparison to images reconstructed by FBP and Hybrid IR, images reconstructed by AIIR display a marked reduction in noise and cone-beam artifact, resulting in a clearer visualization of the large area of cerebral infarction. Additionally, the small blood vessels passing through the infarction can also be clearly seen in images reconstructed by AIIR.

Figure 18. Adult Head Angiography Scanning CT Images

Voltage	Current	CTDIvol	DLP	ED	Slice thickness	Rotation Speed	Scan type
120kV	346mA	48.78mGy	766.8mGy*cm	1.6mSv	0.5mm	1.0s	Axial

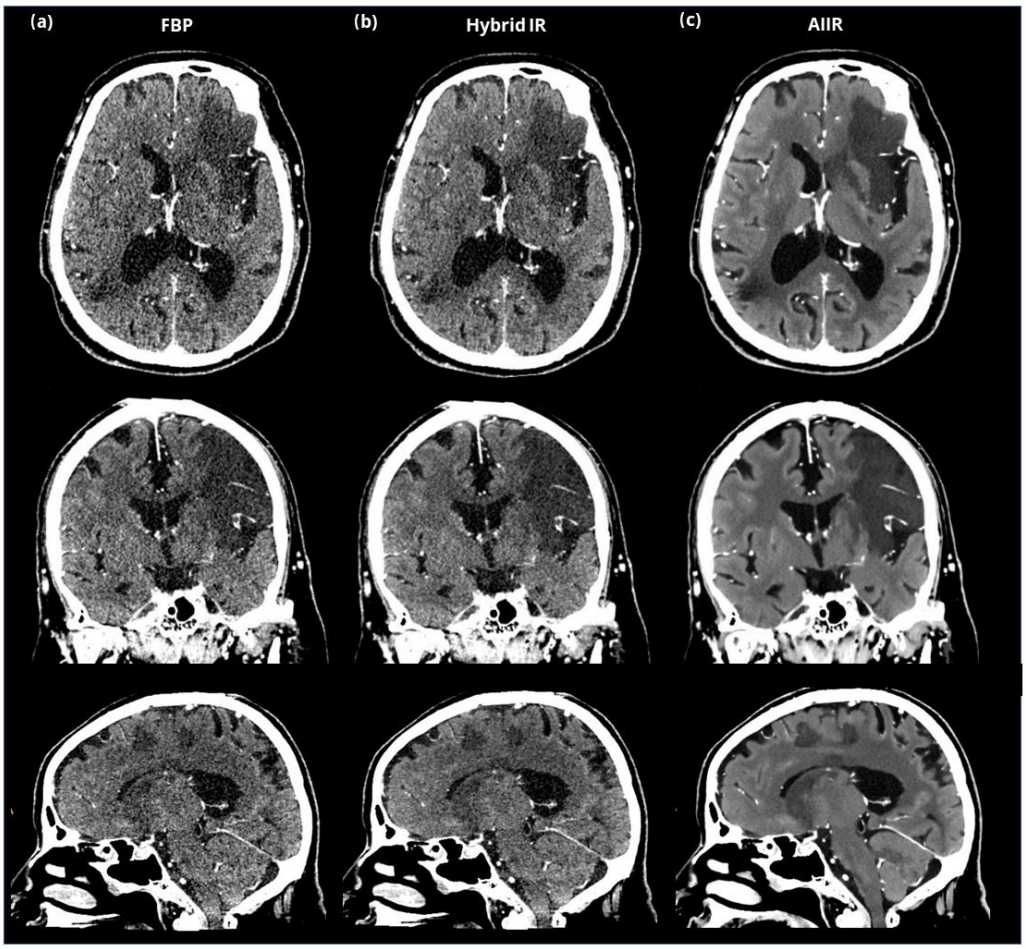

Scan Parameters: 120 kV, CTDIvol=48.78mGy, slice thickness=0. 5 mm, axial scan type

From the left to the right show the results of (a) FBP, (b) Hybrid IR, and (c) AIIR respectively.

Conclusion

In summary, the AIIR reconstruction technology represents a groundbreaking innovation in the field of medical CT imaging, pioneered by United Imaging Healthcare.AIIR seamlessly integrates model-based iterative reconstruction with cutting-edge AI deep-learning technology.By leveraging the strengths of both approaches, AIIR offers a unique combination of robust noise reduction and artifact minimization, allowing for ultra-low-dose CT imaging with outperforming image quality.Additionally, the reconstructed images feature a more realistic image texture, which is highly valued by clinicians. The combination of these two powerful technologies allows AIIR to establish a new standard in low-dose imaging, and optimizing image quality in multiple aspects, such as noise reduction, excellent low-contrast detectability, ultra-high spatial resolution, and artifact-free image performances.Ultimately, AIIR can deliver exceptional image quality and diagnostic capabilities.

References

1. Z.Yu, J.Thibault, C.A.Bouman, K.D.Sauer, J.Hsieh. Fast model-based X-ray CT reconstruction using spatially nonhomogeneous ICD optimization. IEEE Trans Image Process, 20 (2011), pp. 161-175
2. Lu Liu, Model-based Iterative Reconstruction: A Promising Algorithm for Today's Computed Tomography Imaging, Journal of Medical Imaging and Radiation Sciences, Volume 45, Issue 2, 2014, Pages 131-136, ISSN 1939-8654
3. Zeng G L, Wang W. Does Noise Weighting Matter in CT Iterative Reconstruction [J]. IEEE Transactions on Nuclear Science, 2017, 1(1): 68-75.
4. AiCE Deep Learning Reconstruction: Bringing the power of Ultra-High Resolution CT to routine imaging, Kirsten Boedeker. https://us.medical.canon/resources/modals/computed-tomography/aice/white-paper/
5. A new era of image reconstruction: TrueFidelity. Jiang Hsieh, Eugene Liu, Brian Nett. *https://www.gehealthcare.com/-/jssmedia/040dd213fa89463287155151fdb01922.pdf*
6. DELTA white paper. (DELTA is UIH's Deep learning reconstruction product).
7. Sidky E Y, Pan X. Image reconstruction in circular cone-beam computed tomography by constrained, total-variation minimization [J]. Physics in Medicine and Biology, 2008, 53(17): 4777-4807.
8. S.Boyd, N.Parikh, E.Chu, B.Peleato, and J.Eckstein, "Distributed optimization and statistical learning via the alternating direction method of multipliers," Foundations and Trends in Machine Learning, vol.3, no. 1, pp. 1–122, 2010.
9. Ran He, Wei-Shi Zheng, Tieniu Tan, Zhenan Sun, Half-quadratic-based iterative minimization for robust sparse representation, IEEE Trans. Pattern Anal. Mach. Intell. 36 (2) (2014) 261–275
10. Hammernik K, Klatzer T, Kobler E, et al. Learning a variational network for reconstruction of accelerated MRI data.[J]. Magnetic Resonance in Medicine, 2018, 79(6): 3055-3071.
11. You, Y., Zhong, S., Zhang, G.et al. Exploring the Low-Dose Limit for Focal Hepatic Lesion Detection with a Deep Learning-Based CT Reconstruction Algorithm: A Simulation Study on Patient Images. J Digit Imaging. Inform. med. (2024).
12. Computed tomography image quality (CTIQ): low-contrast detectability (LCD) assessment when using dose reduction technology, NEMA/MITA WP 1-2017
13. Yu, Lifeng, Leng, et al. Prediction of human observer performance in a 2-alternative forced choice low-contrast detection task using channelized Hotelling observer: Impact of radiation dose and reconstruction algorithms[J]. Medical Physics, 2013.
14. Kalpana M. Kanal, Priscilla F. Butler, Mythreyi B. Chatfield, et al. U.S. Diagnostic Reference Levels and Achievable Doses for 10 Pediatric CT Examinations Radiology 2022 302:1, 164-174.

Shanghai, China
2258 Chengbei Rd., Jiading District, Shanghai, 201807.

Email | info.global@united-imaging.com

Business Consultation | +86（21）- 67076666

After-sales Service | 4006 - 866 - 088

ABOUT UIH

At United Imaging Healthcare, we develop and produce advanced medical products, digital healthcare solutions, and intelligent solutions that cover the entire process of imaging diagnosis and treatment. Founded in 2011, our company has subsidiaries and R&D centers across China, the United States, and other parts of the world. With a cutting-edge digital portfolio and a mission of Equal Healthcare for All™, we help drive industry progress and bold change.

To learn more, visit https://www.united-imaging.com